

Organometallic Quinonoid Linkers: A Versatile Tether for the Design of Panchromatic Ruthenium(II) Heteroleptic Complexes

Aurélie Damas,[†] Barbara Ventura,[‡] M. Rosa Axet,[†] Alessandra Degli Esposti,[‡] Lise-Marie Chamoreau,[†] Andrea Barbieri,^{*,†,‡} and Hani Amouri^{*,†}

[†]*Institut Parisien de Chimie Moléculaire, UMR 7201, Université Pierre et Marie Curie-Paris 6, 4 place Jussieu, case 42, 75252 Paris Cedex 05, France, and* [‡]*Istituto per la Sintesi Organica e la Fotoreattività (ISOF), Consiglio Nazionale delle Ricerche (CNR), Via Gobetti 101, 40129 Bologna, Italy*

Received October 3, 2010

The synthesis, X-ray structure determination, and photophysical investigation of a novel series of heteroleptic ruthenium(II) polypyridine complexes with organometallic linkers are reported. The displayed panchromatic absorption features are assigned by means of time-dependent density functional theory studies.

The development of clean and renewable energy production technologies is imposed by the limited availability of fossil fuels and the severe environmental problems caused by their combustion. Solar energy is a key resource to meet the rapidly increasing global demand for energy, and it is already cost-competitive with fossil- and nuclear-generated electricity.¹ Dye-sensitized solar cells (DSSCs) based on nanocrystalline porous TiO₂ films are promising devices to generate clean energy as an alternative to the conventional silicon-based photovoltaic devices.² In DSSCs, the sensitizer is one of the critical components because it absorbs sunlight and induces the charge-separation process. Fast charge recombination rates as well as insufficient light absorption are still considered as the key limiting factors for the overall efficiencies of DSSCs. The dyes used in the most efficient DSSCs reported to date³ are typically ruthenium(II) polypyridine complexes with a molar absorption coefficient, ϵ , of around $1 \times 10^4 \text{ M}^{-1} \cdot \text{cm}^{-1}$, usually centered in the green/yellow spectral region, thus exhibiting only poor red/near-infrared (NIR) absorption.⁴ Several strategies have been devised in order to prepare panchromatic absorbers,

such as (i) extending conjugation in the ancillary ligand,⁵ (ii) modifying the ancillary ligand with electron-donating groups,⁶ (iii) using multichromophoric dyes,⁷ and (iv) introducing a new class of cyclometalated ruthenium complexes.⁸

We recently reported the synthesis of organometallic (OM) benzoquinone (bzq) complexes [Cp^{*}M(bzq)] (M = Rh, Ir; Cp^{*} = pentamethylcyclopentadienyl) and their usage as OM linkers for the preparation of a unique type of supramolecular assemblies⁹ with useful luminescent properties.¹⁰ Because this complex-as-ligand approach proved to be very effective in the modulation of the electronic properties of ruthenium(II) polypyridyl complexes, it is useful for the preparation of a novel class of heteroleptic complexes. In this Communication, we report on the synthesis and photophysical characterization of a series of bimetallic heteroleptic ruthenium(II) polypyridine complexes (Chart 1) with extended red/NIR absorption. Here π -bonded ruthenium, rhodium, and iridium *o*-benzoquinone complexes act as chelating units for the [Ru(bpy)₂] moiety. The monometallic sandwich complexes [Cp^{*}M(*o*-bzq)]ⁿ (M = Ru, Rh, Ir) were also prepared for comparison purposes. Density functional theory (DFT) and time-dependent DFT (TD-DFT) calculations of the geometries, the electronic structures, and the singlet electronic transitions have been performed. The results of the theoretical investigation allowed us to shed light on the nature of the dye's excited states.

The binuclear octahedral assemblies were prepared by treatment of the OM linkers and the luminophore [Ru(bpy)₂-(solvent)]²⁺ in acetone. In particular, the anionic OM linker [Cp^{*}Ru(*o*-bzq)]⁻ [Cs] (**Ru2**) was obtained by deprotonation of

*To whom correspondence should be addressed. E-mail: andrea.barbieri@isof.cnrs.fr (A.B.), hani.amouri@upmc.fr (H.A.). Fax: (39)051-6399844 (A.B.), (33)1-44-27-38-41 (H.A.).

(1) (a) Armaroli, N.; Balzani, V. *Energy for a Sustainable World: From the Oil Age to a Sun-Powered Future*, 1st ed.; Wiley-VCH: Weinheim, Germany, 2010; p 356. (b) Armaroli, N.; Balzani, V. *Angew. Chem., Int. Ed.* **2007**, *46*, 52–66.

(2) (a) Gratzel, M. *Nature* **2001**, *414*, 338–344. (b) Gratzel, M. *Acc. Chem. Res.* **2009**, *42*, 1788–1798.

(3) (a) Chiba, Y.; Islam, A.; Watanabe, Y.; Komiya, R.; Koide, N.; Han, L. Y. *Jpn. J. Appl. Phys., Part 2* **2006**, *45*, L638–L640. (b) Nazeeruddin, M. K.; De Angelis, F.; Fantacci, S.; Selloni, A.; Viscardi, G.; Liska, P.; Ito, S.; Bessho, T.; Gratzel, M. *J. Am. Chem. Soc.* **2005**, *127*, 16835–16847.

(4) Nazeeruddin, M. K.; Pechy, P.; Renouard, T.; Zakeeruddin, S. M.; Humphry-Baker, R.; Comte, P.; Liska, P.; Cevey, L.; Costa, E.; Shklover, V.; Spiccia, L.; Deacon, G. B.; Bignozzi, C. A.; Gratzel, M. *J. Am. Chem. Soc.* **2001**, *123*, 1613–1624.

(5) Wang, P.; Klein, C.; Humphry-Baker, R.; Zakeeruddin, S. M.; Gratzel, M. *J. Am. Chem. Soc.* **2005**, *127*, 808–809.

(6) Chen, C. Y.; Wang, M. K.; Li, J. Y.; Pootrakulchote, N.; Alibabaei, L.; Ngoc-le, C. H.; Decoppet, J. D.; Tsai, J. H.; Gratzel, C.; Wu, C. G.; Zakeeruddin, S. M.; Gratzel, M. *ACS Nano* **2009**, *3*, 3103–3109.

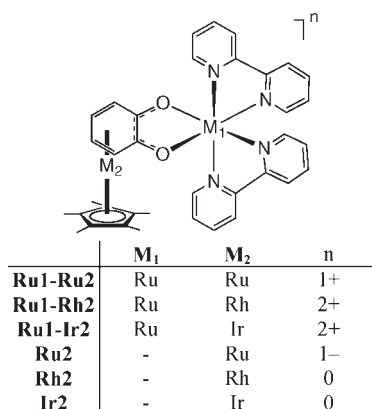
(7) Campbell, W. M.; Burrell, A. K.; Officer, D. L.; Jolley, K. W. *Coord. Chem. Rev.* **2004**, *248*, 1363–1379.

(8) Bessho, T.; Yoneda, E.; Yum, J. H.; Guglielmi, M.; Tavernelli, I.; Imai, H.; Rothlisberger, U.; Nazeeruddin, M. K.; Gratzel, M. *J. Am. Chem. Soc.* **2009**, *131*, 5930–5934.

(9) (a) Moussa, J.; Amouri, H. *Angew. Chem., Int. Ed.* **2008**, *47*, 1372–1380. (b) Moussa, J.; Rager, M. N.; Chamoreau, L. M.; Ricard, L.; Amouri, H. *Organometallics* **2009**, *28*, 397–404.

(10) Moussa, J.; Wong, K. M. C.; Chamoreau, L. M.; Amouri, H.; Yam, V. W. W. *Dalton Trans.* **2007**, 3526–3530.

Chart 1. Schematic Structure of the Investigated Compounds



the catechol ruthenium complex $[\text{Cp}^*\text{Ru}(\text{C}_6\text{H}_6\text{O}_2)][\text{CF}_3\text{SO}_3]^{11}$ with Cs_2CO_3 in CH_2Cl_2 (see the Supporting Information, SI). Subsequent treatment with the solvated ruthenium bipyridine provided the target compound **Ru1–Ru2** in quantitative yield as a burgundy powder. The synthesis of **Ru1–Rh2** and **Ru1–Ir2** was previously described by us.^{9b,12}

The binuclear assembly **Ru1–Ru2** was fully characterized, and in addition single-crystal X-ray diffraction (XRD) was carried out (vide infra). The ^1H NMR spectrum of **Ru1–Ru2** recorded in CD_2Cl_2 showed the presence of 14 multiplets in a range of 6.8–9.4 ppm corresponding to the two nonequivalent bpy ligands, 3 multiplets at 4.9, 4.8 and 4.37 ppm, which are attributed to the coordinated *o*-benzoquinone, and 1 singlet at 1.64 ppm for $\eta\text{-Cp}^*\text{Ru}$. These signals are upfield relative to the free OM linker **Ru2**. Convenient crystals for X-ray study were obtained from $\text{CH}_2\text{Cl}_2/\text{ether}$ via a slow diffusion technique. The X-ray structure of **Ru1–Ru2** (Figure 1) revealed the presence of two independent molecules, a and b, in the unit cell and confirms the O,O' σ -chelating mode of the OM linker **Ru2** to the $\text{Ru}(\text{bpy})_2$ core via both catechol oxygen atoms. The Ru^{II} center is also coordinated to four nitrogen atoms of two bpy ligands, which describes a distorted octahedral geometry around the metal center. The structure also shows that *o*-quinone is coordinated to the Cp^*Ru moiety via the four diene carbon atoms in η^4 fashion. In molecule a, the $\text{Ru2}\text{---C21}$ and $\text{Ru2}\text{---C22}$ distances are 2.31 and 2.41 Å, respectively, indicating the absence of interaction. Further, the $\text{C21}\text{---O1}$ and $\text{C22}\text{---O2}$ bond distances are 1.319 and 1.303 Å, suggesting some double-bond character. Moreover, the two quinone functional groups are bent upward relative to the Cp^*Ru moiety with only 6.37°; this angle is smaller than that reported previously for the $\text{Ru}\text{---Ir}$ octahedral assembly where $\theta = 12.74^\circ$.^{9b} Overall, the structure shows that the OM linker **Ru2** has some catecholate resonance contribution rather than a pure *o*-bzq form (Chart 1).⁹

The absorption spectra of all investigated complexes and the reference $[\text{Ru}(\text{bpy})_3]^{2+}$ (**Ru**) are reported in Figure 2; the relevant photophysical data are summarized in Table 1. The monometallic complexes **Rh2** and **Ir2** show only high-energy electronic transitions of modest intensity (see Table 1), while no absorption in the visible is present. The bimetallic complexes **Ru1–Ru2**, **Ru1–Rh2**, and **Ru1–Ir2** exhibit quite dif-

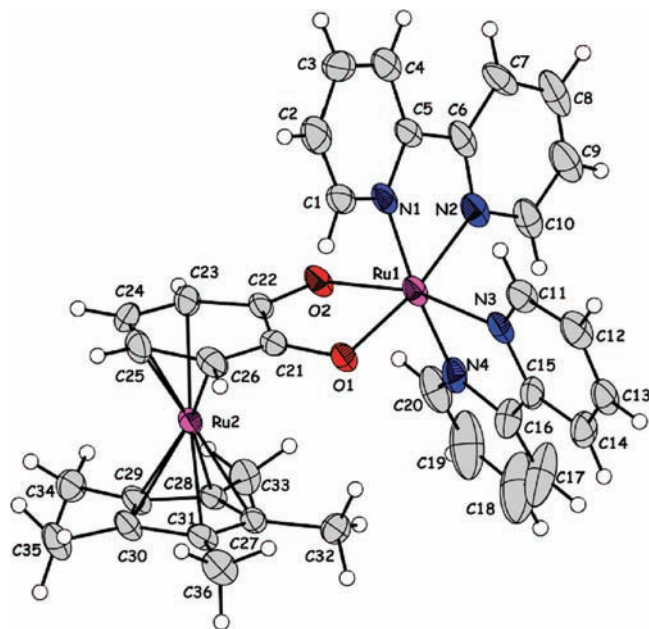


Figure 1. Molecular structure of the cationic part of **Ru1–Ru2** at 30% ellipsoids with atom labeling. Only molecule a is shown.

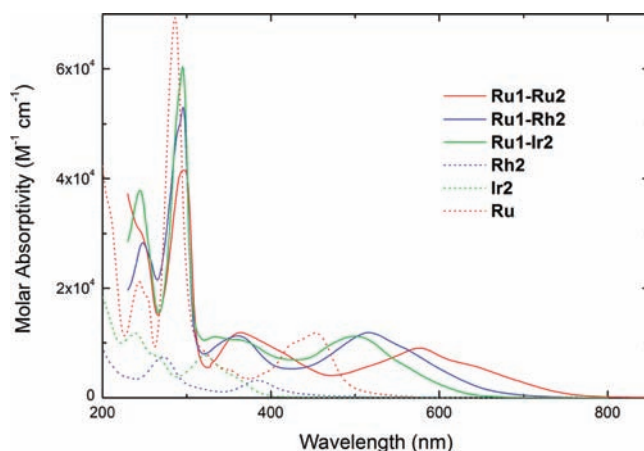


Figure 2. Absorption spectra of complexes in CH_2Cl_2 solutions. The spectrum of **Ru** in a H_2O solution is reported as a reference.

ferent spectral shapes. Their absorption spectra display three main features, in order of decreasing energy: (i) two intense bands in the UV region of the spectrum, located around 245 and 290 nm, which are also present in the reference compound **Ru** at comparable energies and intensities, usually assigned to bpy-centered $\pi\text{---}\pi^*$ transitions;¹³ (ii) a mid-energy band at ca. 360 nm, with ϵ values larger than $1 \times 10^4 \text{ M}^{-1}\cdot\text{cm}^{-1}$; (iii) a high-intensity, low-energy band, whose energy is modulated by the metal M_2 in the OM linker (see Chart 1). This last band is responsible for the panchromatic behavior of this novel class of heteroleptic ruthenium(II) polypyridine derivatives. In fact, the band maxima span from 500 to 580 nm in passing from $\text{M}_2 = \text{Ir}, \text{Rh}$, and Ru , with a shoulder at 640 nm ($\epsilon \approx 6000 \text{ M}^{-1}\cdot\text{cm}^{-1}$) and a long tail extending beyond 700 nm in the latter case (Figure 2). Overall, it represents a clear improvement over the absorption features of the best-performing dyes for DSSCs (see a comparison in the SI).^{3b,4} The spectral features

(11) (a) Moussa, J.; Guyard-Duhayon, C.; Herson, P.; Amouri, H.; Rager, M. N.; Jutand, A. *Organometallics* **2004**, *23*, 6231–6238. (b) Vichard, D.; Gruselle, M.; Amouri, H.; Jaouen, G. *J. Chem. Soc., Chem. Commun.* **1991**, 46–48.

(12) Damas, A.; Moussa, J.; Rager, M. N.; Amouri, H. *Chirality* **2010**, *22*, 889–895.

(13) Campagna, S.; Puntoriero, F.; Nastasi, F.; Bergamini, G.; Balzani, V. *Top. Curr. Chem.* **2007**, *280*, 117–214.

Table 1. Photophysical Parameters of the Investigated Compounds

	absorption (RT) ^a		emission (77 K) ^b	
	λ_{max} , nm (ϵ_{max} , M ⁻¹ ·cm ⁻¹)		λ_{max} , nm	τ , μs
Ru1–Ru2	247 (29.9 × 10 ³), 297 (41.5 × 10 ³), 363 (11.8 × 10 ³), 578 (9.0 × 10 ³)		768	1.2
Ru1–Rh2	248 (28.4 × 10 ³), 296 (53.0 × 10 ³), 362 (11.2 × 10 ³), 517 (11.9 × 10 ³)		692	1.1
Ru1–Ir2	245 (37.8 × 10 ³), 295 (60.4 × 10 ³), 360 (10.6 × 10 ³), 500 (11.2 × 10 ³)		698	1.3
Ru	244 (21.8 × 10 ³), 287 (73.7 × 10 ³), 450 (12.7 × 10 ³)		590	4.1
Rh2	272 (7.5 × 10 ³), 383 (3.2 × 10 ³)		nd	nd
Ir2	239 (11.8 × 10 ³), 322 (7.7 × 10 ³)		567	nd

^a In a dichloromethane solutions, but with **Ru** in water. ^b In a 1:4 MeOH/EtOH mixture. nd is not detected.

in the visible range displayed by these bimetallic derivatives are rather different from those of the reference complex **Ru**, which only shows a series of electronic transitions located around 450 nm of $d_{\text{Ru}} \rightarrow \pi^*_{\text{bpy}}$ metal-to-ligand charge-transfer (MLCT) nature.¹³

In order to get further insight into the nature of the excited states, the transitions energies, wavelengths, and oscillator strengths (f_{osc}) have been calculated and are reported in Table 1 in the SI. The simulations of the excitation spectra (Figure 1 in the SI) satisfactorily reproduce the spectral features of the low-energy absorption bands observed in the bimetallic complexes (Figure 2). All electronic transitions contributing to this band originate from the three highest occupied molecular orbitals (MOs; Table 1 in the SI). Inspection of the electronic distribution of the frontier orbitals reveals that the different OM linkers have a more significant influence on the virtual MO distribution than on occupied MOs (Figure 2 in the SI). Calculations show that the three highest occupied MOs of all bimetallic complexes are mainly of d_{Ru1} character with some π_{bzq} contribution, especially in the case of the homobimetallic ruthenium derivative. The situation differentiates for the virtual orbitals (VOs): (i) for **Ru1–Ru2**, the first five VOs are clearly localized on the bpy ligands; (ii) for **Ru1–Rh2**, the lowest unoccupied MO (LUMO) is localized on the OM linker, which also contributes to the next two VOs, whereas the bpy-centered π orbitals lie at higher energies (Figure 2 in the SI) although still contributing to the formation of the low-energy excitation band (Table 1 in the SI); (iii) for **Ru1–Ir2**, the LUMO and LUMO+1 distributions are similar to those observed for **Ru1–Ru2** though, as for **Ru1–Rh2** but to a lesser extent, the OM linker participates in their description. Thus, the low-energy absorption band can be assigned to the $d_{\text{Ru1}} \rightarrow \pi^*_{\text{bpy}}$ transition of $\text{ML}_{\text{bpy}}\text{CT}$ character with minor contributions from (i) $\pi_{\text{bzq}} \rightarrow \pi^*_{\text{bpy}}$ transitions of $\text{L}_{\text{bzq}}\text{L}_{\text{bpy}}\text{CT}$ character for **Ru1–Ru2** and (ii) $d_{\text{Ru1}} \rightarrow \pi^*_{\text{bzq}}$ transitions of $\text{ML}_{\text{bzq}}\text{CT}$ character for **Ru1–Rh2** and **Ru1–Ir2**. The calculated electronic charge distribution (Table 2 in the SI) indicates that in the **Ru1–Ru2** ground state the OM linker has a larger attitude to attract electrons from the $\text{Ru}(\text{bpy})_2$ moiety with respect to the other two complexes, which favors $\text{L}_{\text{bzq}}\text{L}_{\text{bpy}}\text{CT}$ transitions. In the case of **Ru1–Rh2**, the contribution from $\pi_{\text{bzq}} \rightarrow \pi^*_{\text{bzq}}$ transitions, which reduces the CT character of the band, should also be taken into account.

The investigated complexes showed faint (**Ru1–Ir2**) or no emission at room temperature in CH_2Cl_2 solutions, while an intense emission is observed in a glassy matrix at 77 K for all bimetallic complexes (Figure 3). For the case of the monometallic **Ir2** complex, only a weak emission is observed at 77 K, while no emission has been detected for **Rh2** (see Table 1). Notably, all bimetallic complexes show a bright NIR emission of ³CT nature.

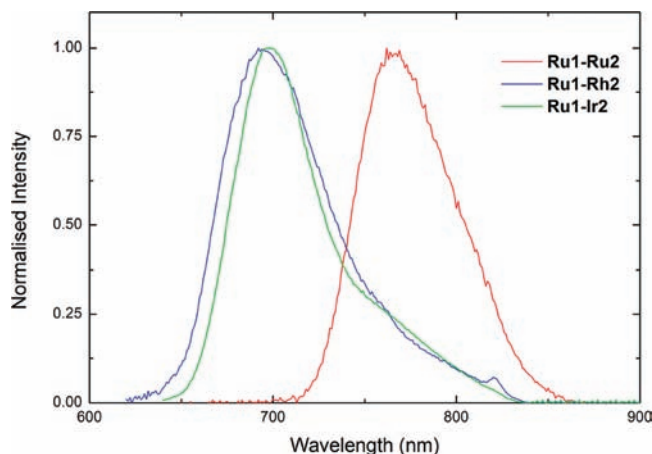


Figure 3. Emission spectra of bimetallic complexes in MeOH/EtOH (1:4, v/v) glassy solutions at 77 K.

In conclusion, we have presented here a combined experimental and theoretical study of a novel series of supramolecular assemblies based on OM quinonoid linkers. These have been synthesized and fully characterized, and for **Ru1–Ru2**, the XRD structure is reported. Notably, this series of panchromatic sensitizers shows improved absorption features with respect to the dyes used in the most efficient DSSCs reported to date. In particular, **Ru1–Ru2** displays an intense absorption band peaking at 580 nm with a shoulder at 640 nm ($\epsilon \approx 6000 \text{ M}^{-1} \cdot \text{cm}^{-1}$) and a long, still fairly intense tail extending beyond 700 nm. The photophysical results have been rationalized by means of TD-DFT studies, allowing us to assign the main spectral features of the dyes. The low-energy absorption band shows mainly a CT character, although some contributions from $\pi-\pi^*$ transitions in the case of **Ru1–Rh2**, and to a lesser extent of **Ru1–Ir2**, which reduce the CT character of the band, should also be taken into account.

Acknowledgment. Funding from the Italian CNR (Project PM.P04.010 “MACOL”) and MIUR (FIRB Projects RBI-P0642YL “LUCI” and RBIP0642YL “NODIS”) and from the French CNRS and UPMC-Paris 6 is acknowledged.

Supporting Information Available: General experimental and spectroscopic methods, synthesis of ligands and complexes, crystallographic data (CIF and additional structural data), and computational details. This material is available free of charge via the Internet at <http://pubs.acs.org>.

Note Added after ASAP Publication. This paper was published on the Web on November 1, 2010, with a minor text error. The corrected version was reposted on November 4, 2010.